AN EVALUATION OF A PARALLEL-RESONANT

CURRENT-SOURCE CONVERTER

FOR AN ELECTROTHERMAL THRUSTER

A Thesis

by

ARISTIDE-MARIE TCHAMDJOU

Submitted to the Office of Graduate Studies of
Texas A&M University
in partial fulfillment of the requirements for the degree of

MASTER OF SCIENCE

December 1996

Major Subject: Electrical Engineering

AN EVALUATION OF A PARALLEL-RESONANT

CURRENT-SOURCE CONVERTER

FOR AN ELECTROTHERMAL THRUSTER

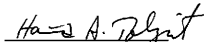A Thesis

by

ARISTIDE-MARIE TCHAMDJOU

Submitted to Texas A&M University
in partial fulfillment of the requirements
for the degree of

MASTER OF SCIENCE

Approved as to style and content by:

Mehrdad Ehsani
(Chair of Committee)

Hamid Toliyat
(Member)

N. Kehtarnavaz
(Member)

Frederick Best
(Member)

A. D. Patton
(Head of Department)

December 1996

Major Subject: Electrical Engineering

ABSTRACT

An Evaluation of a Parallel-Resonant Current-Source Converter

for an Electrothermal Thruster. (December 1996)

Aristide-Marie Tchamdjou, Diplom, Technische Universitaet Berlin

Chair of Advisory Committee: Dr. Mehrdad Ehsani

The Parallel-Resonant Current-Source Converter promises highly efficient DC-DC power conversion. It uses zero-voltage switching to reduce the losses and improve the converter efficiency. The Parallel-Resonant Current-Source Converter has been developed from an idea of Dr. Ehsani from Texas A&M and Dr. Pitel from Magna-Power Electronics, Inc.. It is primarily intended for space applications, where efficiency, reliability and size are traditionally important. The reliability of the converter is increased by the current-source characteristics of the input and the minimum device count. The converter falls under the classification of resonant converters, which are gaining importance due to ever increasing demands on converter size and efficiency. Although wide application of resonant-mode converters is handicapped by the complexity in control when compared to PWM converters, they are perfectly suitable for some specific applications. Improvement in control and sensing devices will render resonant technology more attractive in the future.

........*To my parents,*

      my family,

      my friends,

      and all my teachers...

ACKNOWLEDGMENTS

TABLE OF CONTENTS

LIST OF FIGURES

LIST OF TABLES

CHAPTER I

INTRODUCTION

For many years, power conversion has posed a great challenge to engineers. Meanwhile it has evolved into a multi-disciplinary technology [1]. Power supplies are inseparable parts of electric appliances and equipment today. Electric appliances require supply voltages which are not always compatible with the available power source. A special unit, the power supply, must then convert the source energy into a form suitable for the appliance. Power supplies used to be regarded as familiar black boxes, but today they are often an integrated subassembly, especially in the lower power range. The basic engine of modern power supplies is the power electronics converter.

This thesis presents a new DC-DC converter topology, the Parallel-Resonant Current-Source Converter (Fig. 1) . Its principle of operation is based on the hard-switched Current-Source Converter [2]. It uses resonant techniques to reduce the overall losses and improve the efficiency. Soft-switching permits an increase of operation frequency, which in turn reduces the size of the converter.

A. Evolution of Power Supply Technology

The advent of the transistor was an important milestone in the development of contemporary solid-state power supplies [3]. In the past, the complexity of power

---

The journal model for this thesis is *IEEE Transactions on Power Electronics*.
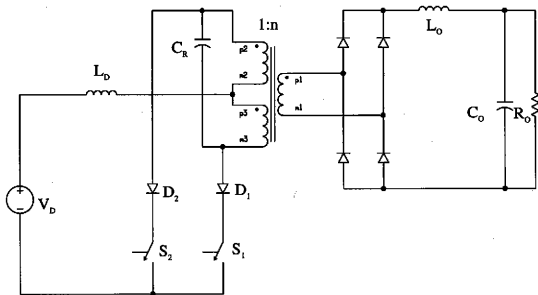
Fig. 1. The Parallel-Resonant Current-Source Converter.

supplies arose because electric appliances required different voltage levels for subcircuits which performed different tasks. Several power supplies delivering the voltage required by each subcircuit had to be designed. The general-purpose power supply became a reality with the appearance of solid-state circuits. Transistors used in those early circuits were operated in the linear region. These circuits are thus referred to as linear power supplies.

Although performance and reliability of power supplies increased as years passed, their size remained unchanged because they still depended on the principle of linear regulation, which exhibits a very poor efficiency [2]. Their big share in the overall volume of the equipment they powered prevented the construction of miniature

appliances. The power supply then became the logical starting point for reducing the size and weight of electric equipment.

The switched-mode power supply is the first major step towards the trend of smaller and lighter power supplies. DC-DC converters, the heart of modern DC power supplies, can be regarded as DC voltage transformers. They are developed from the basic topologies of the buck (step-down), boost (step-up) or buck-boost converter. They consist in their elementary form of a diode, an inductor and a turn-off semiconductor device which is operated at high frequency. High frequency of operation reduces the size of bulky elements such as inductors and transformers, which traditionally have a big share in the overall volume of power supplies [2,4,5]. But the quest for high frequency of operation has caused the resurgence of another important aspect of power conversion: the efficiency.

The reduction of the size of switched-mode power supplies by increase of switching frequency is not without penalty. High frequency produces high switching losses which significantly degrade the converter efficiency. The demand for smaller and more efficient power supplies has triggered intense investigation of soft-switched converters. Although resonant technology is well established in high power SCR motor drives and uninterruptible power supplies (UPS), its application in the middle to low power DC-DC converters is a relatively recent phenomenon. Resonant power conversion has not yet established itself as a mature technology because of the complexity in control [6].

B. Basic Features of the Parallel-Resonant Current-Source Converter

Soft-switched converters are broadly classified as quasi-resonant converters and resonant converters . Quasi-resonant converters use the resonant circuit only to create

zero-voltage or zero-current conditions whereas in resonant converters, the resonant tank is an integral part of the power transfer mechanism [4]. Quasi-resonant converters were developed as a way to reduce the high devices stresses common in resonant converters.

Two basic classes of resonant converters exist: the current-fed converter and the voltage-fed converter. In a voltage-fed converter, the DC supply voltage is first chopped into a high-frequency square voltage, then fed into a resonant LC circuit to produce a resonance. The Parallel-Resonant Current-Source Converter falls into the category of current-fed converters; a choke inductor is connected in series with the DC voltage source to simulate a current-source. The current-source is switched between the ground and a parallel LC circuit to induce a high-frequency resonance. The resonant variables are transformed-coupled and rectified to provide a DC output.

The decision for a particular converter is motivated by factors as varied as size, efficiency, ease of control, reliability, cost, etc....The Parallel-Resonant Current-Source Converter is primarily designed for space applications, where efficiency, size and reliability are traditionally important. Analysis of the Parallel-Resonant Current-Source Converter will show that output to input voltage ratio is solely determined by the turn ratio of the transformer for operation at the resonant frequency. Devices stresses and transformer ratings are limited to reasonable levels while device count is minimized. The minimum number of devices increases the reliability of the converter. The fact that both active switches are connected to the ground considerably simplifies their gate-or base drive circuitry.

High converter efficiency is achieved with zero-voltage switching. The high frequency of operation resulting from the low switching losses allows a reduction of the size of the converter [7]. The current-source characteristics of the input provides a natural protection against short-circuit and further improves the reliability of the converter.

Instead of a pulsating current as it is the case with voltage-source converters, current-source converters inject a constant current into the energy source. Further, the parallel structure of the resonant tank restricts the oscillating current in the tank. In series-resonant converters, the resonant current, which can have a high peak value, flows in either the source or the load and produces additional conduction losses. Finally electric isolation is elegantly achieved with a transformer whose magnetizing inductance is also used as the resonant inductance of the LC tank. The size of the center-tapped transformer is reduced by the high frequency of operation.

Digital computer simulation and experimental results on a prototype verify design equations derived in this thesis. The waveforms from the simulation and the experimental setup show the occurrence of zero-voltage switching. The high efficiency predicted by the resonant topology is confirmed by measurements performed on the prototype.

C. Thesis Organization

Chapter II gives a brief overview of linear and switched-mode power supplies while Chapter III explains the basic principles of soft-switching and hard-switching. Benefits and shortcomings of both techniques are compared. The Parallel-Resonant Current-Source Converter is presented in Chapter IV. The principle of operation is explained and the analysis of the circuit is done in the time as well as in the frequency domain. Also design equations for this converter are derived. Chapter V shows simulation results of a design example while Chapter VI presents experimental results obtained with the prototype. The thesis concludes in Chapter VII with a summary and conclusions of the work. A critique of the analysis is done in Chapter VII, which also expands to the impacts of resonant technology in the design of future power converters.

CHAPTER II

CONVENTIONAL POWER SUPPLIES

Switched-mode technology has established itself as the standard in modern DC power supplies. Switched-mode power supplies have penetrated even the low power range, traditionally the domain of linear power supplies. However linear power supplies still have a significant presence in electric equipment.

A. Linear Power Supplies

Linear power supplies still occupy a considerable portion of IC appliances today [3]. Fig. 2 shows the schematic of a simplified linear power supply. A transistor operating in the active region is the main element of the power supply. The output voltage is compared to a reference value and the error is fed to a control circuit that drives the transistor. The transistor operates mainly in the linear region and acts as an adjustable resistor. The voltage difference between input and output appears across the transistor and causes power losses. Operation in the linear region incurs a significant amount of conduction power losses. Overall efficiency of linear power supplies is poor and lies in the range of 30%-60% [2]. When power is drawn from an AC source, a bulky 60 Hz transformer is needed, and the size of the power supply increases. However, linear power supplies utilize simple circuitry and are cheaper in the very low power range [2]. Furthermore they do not produce electromagnetic interference (EMI) with other equipment.
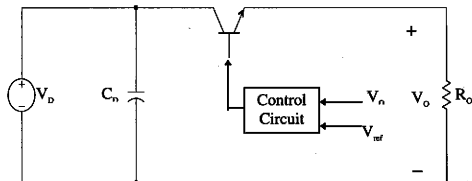
Fig. 2. Simplified Linear Power Supply.

B. Switched-Mode Power Supplies

Switched-mode power supplies use electronic switches to process electric power. The semiconductor devices are either "fully on" or "fully off". When "fully on", the device operates in the saturation region where voltage is low. Power dissipation in the semiconductor devices is reduced. Switched-mode power supplies have a better efficiency than linear power supplies [2].

The DC-DC converter is the heart of switched-mode power supplies. In their most elementary form, DC-DC converters appear in 3 basic topologies: buck or step-down converter, boost or step-up converter and buck-boost converter. Each of the 3 basic topologies consists of a diode, a turn-off semiconductor device, an inductor and a capacitor. Most switched-mode DC-DC converters are developed from those 3 basic topologies.

Currents and voltages in a switched-mode power supply have a trapezoidal/square/ triangular shape. Hence they are referred to as square-wave converters. The basic equations of buck, boost and buck-boost are presented in the following segments. It is assumed that the converters are in steady-state, the circuit elements are ideal and the mode of conduction is continuous.

D is the switch duty cycle and T the switching period.

$$D = \frac{t_{on}}{t_{on} + t_{off}} = \frac{t_{on}}{T} \qquad (2.1)$$

1. The Buck Converter
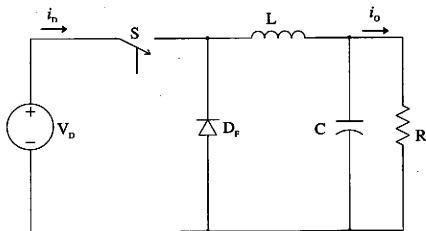
Fig. 3. Buck Converter.

The buck converter is fed by the input voltage V_D and produces the output voltage V_o. During normal operation, the switch S is driven on and off by a pulse-width modulator (PWM). When S is on, current increases linearly in the inductor and energy is stored in it. Is S turned off, the energy stored in the inductor forces the current to flow through the "flywheel" diode D_F. The flywheel diode must provide a path for the inductor current at turn-off of S since inductors do not allow current jumps.

The output to input voltage ratio of a buck converter (Fig. 3) in continuous conduction mode is:

$$\frac{V_o}{V_D} = D \qquad (2.2)$$

The output voltage can be varied between 0 and V_D. Output voltage is always lower than input voltage. The output voltage ripple [2] is given by:

$$\Delta V_o = \frac{V_o^2}{8CLf_s^2}(1-D) \qquad (2.3)$$

2. The Boost Converter

While S is on, current increases linearly in the inductor L. Meanwhile magnetic energy is stored up. Is S turned off, the inductor current decreases because a higher load is being connected across the input circuit. The energy delivered by the source adds to the energy that was stored in L and is transferred to the output. Since the supply energy is added to the inductor energy to charge up the output capacitor, the output voltage V_o is larger than the input voltage V_D.
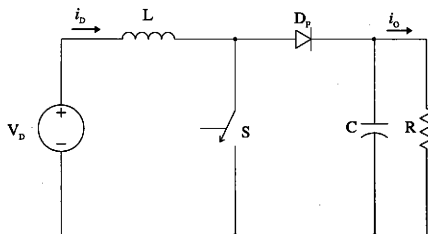
Fig. 4. Boost Converter.

Fig. 5. Buck-Boost Converter.

The output to input voltage ratio of the boost converter (Fig. 4) in continuous conduction mode is :

$$\frac{V_o}{V_D} = \frac{1}{1-D}$$
(2.4)

Output voltage V_o is always larger than the input voltage V_D since $0 \leq D \leq 1$. For an average output current I_o, the output voltage ripple [2] is given by:

$$\Delta V_o = \frac{I_o}{Cf_s} D$$
(2.5)

3. The Buck-Boost Converter

When S is turned on, current builds up linearly in the inductor L while energy is stored in it. During that mode, the output capacitor alone supplies energy to the output. The output capacitor of the buck-boost must therefore be rated high enough. When S is turned off, the inductor current forces its way through the flywheel diode D_F, charging up the output capacitor C. Because the flow of the current I_L is now opposed by the output voltage V_o, I_L decreases linearly.
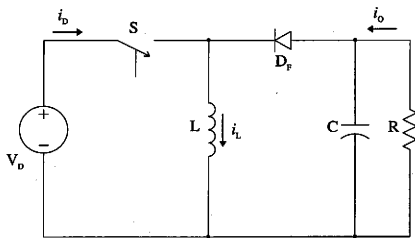
The output to input voltage ratio of a buck-boost converter (Fig. 5) in continuous conduction mode is:

$$\frac{V_o}{V_D} = \frac{D}{1-D}$$
(2.6)

This converter can step up or step down the voltage. For a given output current I_o, the ripple in the output voltage [2] is:

$$\Delta V_o = \frac{I_o}{Cf_s} D \qquad (2.7)$$

Other square-wave converters are derived from the 3 basic topologies. For example the Cuk converter (Fig. 6) is a cascaded connection of a boost converter followed by a buck converter (Fig. 7). The cascaded nature of the connection is reflected in the output to input voltage ratio, which is the same as for the buck-boost converter.

The switching frequency has no direct influence on the voltage ratio of switched-mode converters in continuous conduction mode (equations 2.2, 2.4 and 2.6). But it has an effect over the mode of conduction. Low switching frequency transfers the converter into discontinuous conduction. Furthermore, a high switching frequency reduces currents and voltages ripple and produces cleaner DC outputs.

C. DC-DC Converters with Transformer Isolation

According to equations 2.4 and 2.6 , ideal boost and buck-boost converters produce an infinite output voltage for duty cycles around 100%. But in practice electric parts such as semiconductor devices, inductors and capacitors have parasitic resistances that considerably degrade the voltage ratio of converters. Instead of infinite, the voltage ratio for real converters is nearly zero at maximum duty cycle [8]. Moreover, maximum voltage ratio hardly exceeds 4. A transformer then becomes necessary for significant changes of voltage level.
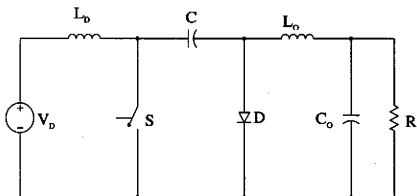
Fig. 6. Cuk Converter.
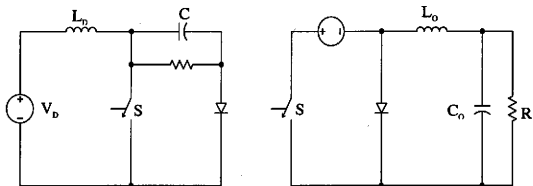
Fig. 7. Cuk as Cascaded Connection of Boost and Buck Converters.

In addition to changing voltage levels , transformers provide electric isolation between input and output, or between the power source and the appliance. An increasing number of equipment contain sensitive electronics that must be protected from "contingencies" on the input side. Electric isolation is essential for power supplies that are connected directly to the ac mains via a rectifier. Transformers also connect multiple isolated outputs to a single input and so eliminate the need for multiple converters. A transformer can simultaneously assume the functions of electric isolation, power bus and voltage level shifter.

Proper operation of a converter with transformer involves balanced drive of the transformer primary [9]. In the absence of balanced drive, a net DC current flows in the transformer primary, causing easy saturation of the core during alternate half-cycles. A DC-DC converter with transformer isolation has many stages (Fig. 8) : the first stage, an inverter, transforms the DC input into an AC voltage across the transformer primary. The second stage, the transformer, provides isolation and voltage level shifting. The AC voltage is reflected on the secondary side and passed through the third stage, a rectifier, to obtain a DC output. The size of the transformer can be reduced when the frequency of the intermediate AC voltage is high.

High-frequency transformers do not seriously alter the low frequency behavior of a converter, but they may change the switching waveforms and complicate the design of the converter. Inductive shunting current due to the existence of primary inductance is another negative side-effect of high frequency transformers [4].

The most visible drawback however is the occurrence of large voltage spikes during switching. It is virtually impossible to build a transformer without leakage inductances. Leakage inductances combined with high rate of change of current produce overvoltages. This phenomenon is particularly severe at high switching

frequencies. Furthermore the transformer incurs non negligible eddy-current, copper and hysterisis losses at high frequency.
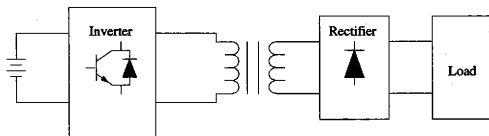
Fig. 8. DC-DC Converter with Transformer Isolation.

CHAPTER III

HARD-SWITCHING VERSUS SOFT-SWITCHING

A. The Ideal Switch

In the analysis of converters in Chapter II, it is quietly assumed that switches are ideal. Ideal switches have zero voltage drop in on-state. Furthermore, switching transitions occur very fast. Ideal switches do not incur any losses during conduction, nor during switching (Fig. 9) . Thus the ideal switch can be operated at unlimited frequency.
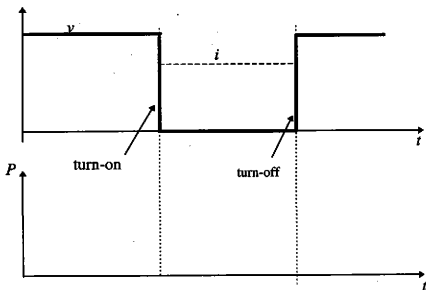
Fig. 9. Turn-on and Turn-off of an Ideal Switch.

B. The Real Switch

In power electronics, switches are realized with semiconductor devices. A real switch has a forward resistance, which causes a non-zero voltage drop during conduction. Also, switching takes place in finite times. For a short duration, current flowing through the switch and voltage across it take simultaneously high instantaneous values. Switching losses are so generated (Fig. 10). This mechanism is repeated at each switching transition. Switching losses are proportional to switching frequency. Operation at high frequency generates high switching losses and degrades the overall efficiency of the converter.
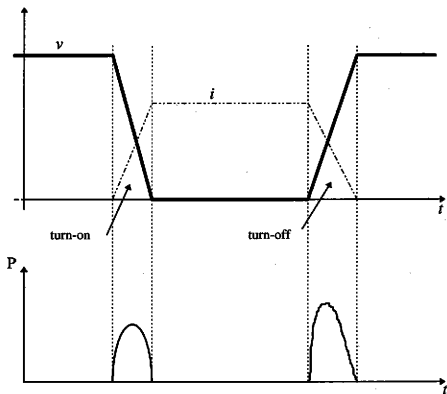
Fig. 10. Turn-on and Turn-off of a Real Switch.

C. Problems of PWM Power Conversion

Semiconductor devices like MOSFETs and IGBTs have short switching times which permit high frequency of operation [10]. High switching frequency reduces the size of the converter, but also has undesirable side-effects like high switching losses, leakage spikes and charge dumping [5].

In a switched-mode converter, switching waveforms are typically rectangular, with abrupt transitions and nearly vertical edges. The presence of leakage inductance in transformers and board wiring in combination with sharp di/dt causes voltage spikes at turn-off. These voltage spikes can easily damage semiconductor devices in the circuit. Furthermore oscillatory spike waveforms are a source of noise. In practical circuits, snubbers are used to prevent dangerous overvoltage and reduce the power dissipated in semiconductors. Snubbers protect devices by diverting a portion of the losses away from the devices to other circuit elements [11]. But the total amount of energy dissipated in the switch-snubber combination does not change much, while the circuit becomes more complex.

Further, energy stored in the junction capacitance of the semiconductor device is trapped and dissipated inside the device at turn-on [5]. While not severe at lower switching frequencies, the capacitive turn-on loss due to discharging of the parasitic junction capacitance of power MOSFETs and IGBTs becomes a dominating factor if the switching frequency is raised to higher levels.

Power semiconductor devices in a switched-mode converter operate between 2 states: "fully on" or "fully off". During state transitions, the power electronic switch is turned on or off from a stiff bus voltage or a stiff current. At switching, high voltage and high current overlap and produce switching losses. Switching losses are not an important factor at low frequency of operation. However they have a negative effect

on the converter efficiency when the switching frequency is raised up to a certain level. With hard-switching, high efficiency and drastic reduction of the converter size can not be achieved simultaneously. The design of hard-switched converters is always a trade-off between those 2 contradictory objectives.

D. Soft-Switched Converters

In contrast to PWM converters, soft-switched converters have waveforms that contain pieces of sinusoidal, ringing profile. Soft-switched converters utilize the presence of inductive and capacitive elements in the circuit to shape waveforms that go through natural zero-crossings. Switches are turned on or off at the zero-crossing with virtually no losses. The switching frequency can be raised without any severe penalty on converter efficiency.

1. Resonant Switches

In resonant converters, electronic commutation is achieved with resonant switches. Resonant switches consist of a main semiconductor device S and auxiliary resonant elements L_R and C_R . The resonant elements L_R and C_R shape the device current or voltage waveforms such that they pass through a natural zero. At the zero-crossing, the device can be turned off or on. When the transition occurs at the zero-crossing of the voltage, it is zero-voltage switching. When it occurs at the zero-crossing of the current, it is zero-current switching. Some converters use zero-current turn-on and zero-voltage turn-off in the same switching cycle.

Voltage-Mode Resonant Switch

In a voltage-mode resonant switch (Fig. 11), the resonating capacitor is connected across the switch. In on-state, the switch acts as a clamping device and maintains the capacitor voltage at zero. When the switch is turned off, the voltage across the parallel connection starts to rise, but can not change instantaneously because of the capacitor. Voltage rises smoothly from zero, in a continuous fashion (Fig. 12) .

Current-Mode Resonant Switch

The resonating inductor is connected in series with the semiconductor device (Fig. 13). In off-state, no current flows in the inductor. When the switch is turned on, current rises from zero to its final value in a smooth and continuous fashion (Fig. 14). Current can not change instantaneously because of the inductor connected in series.

2. Features of Resonant Power Conversion

High efficiency, small size, low weight and reduced acoustic noise are requirements of a good power converter. Manufacturers of power devices contribute to this trend by fabricating devices that switch faster and have higher power rating. The ultimate goal is to achieve a high power density of the converter. High frequency operation reduces the size of reactive elements and transformers, but also generates high switching losses. With resonant power conversion, switching is lossless. The frequency of operation can be raised without seriously degrading the overall efficiency of the converter [12,13].
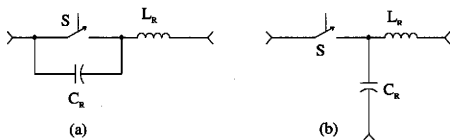
Fig. 11. Voltage-Mode Resonant Switches.
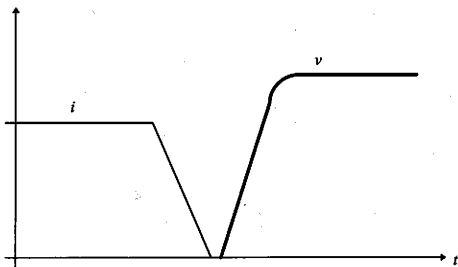
Fig. 12. Turn-off of Voltage-Mode Resonant Switch.
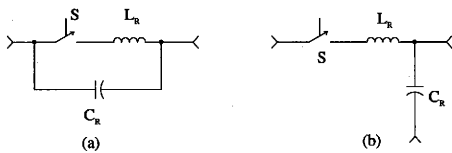
Fig. 13. Current-Mode Resonant Switches.
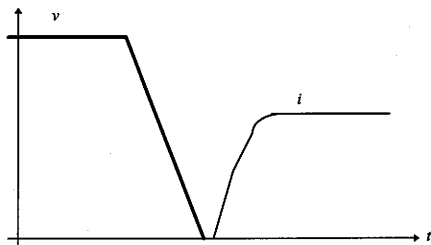
Fig. 14. Turn-on of Current-Mode Resonant Switch.

High switching frequency reduces the requirements for peak energy stored in inductors and capacitors. The converter is then designed with smaller reactive elements. Moreover, the bandwidth of switching regulators is limited to less than half the switching frequency [2]. Operation at high frequency increases the bandwidth and renders transient responses faster [5]. Also the harmonics content of the waveforms is sharply reduced.

Further, resonant power conversion eliminates typical problems associated with PWM converters such as leakage spikes and charge dumping. Leakage spikes and charge dumping are caused by the discontinuity of the waveforms of PWM converters and the high rate of change of voltage and current at switching. Soft-switching on the contrary produces smooth and slowly varying curves which make the presence of parasitic reactances "inoffensive". In fact, parasitic reactances can be constructively included in the design of the reactive elements. Resonant power conversion turns the problem of high leakage inductance into no problem at all.

E. Devices Stresses

Resonant converters suffer from high current and voltage stresses. Typically, resonant waveforms have higher peaks and rms values than PWM waveforms of same average values [5]. Consequently, utilization factor of semiconductor devices is poor and conduction losses higher. The decision for a resonant converter is an optimal choice if the reduction in switching losses far outweighs the increase in conduction losses.

Quasiresonant converters have been developed to eliminate the problems associated with high devices stresses in resonant converters. Devices stresses in quasiresonant converters are similar to those in PWM converters.

F. Analysis and Control

Averaging techniques provide powerful tools to analyze PWM converters and derive equivalent circuit models. However they fail for resonant converters. Analysis of resonant converters can be very complex and in most cases yields results that do not give meaningful insights to the circuit.

Power conversion in resonant converters is load dependent. Control variables must be changed as the load varies. Usually resonant converters have multiple operating modes. A control scheme optimized for a particular mode may perform poorly if a load change forces the converter into another mode. The load range is therefore considerably reduced.

One significant drawback of resonant power conversion is the loss of degrees of freedom compared to a PWM converter with equal number of switches [5]. One switching transition (either turn-on or turn-off) is determined by the control circuit while the other is set by the converter waveforms. In a resonant converter, the choice of reactive elements heavily influences resonant frequency and switching sequence. The versatility in control offered by PWM is not possible with resonant power conversion. The implementation of constant frequency control with a resonant converter is very complex.

CHAPTER IV

THE PARALLEL-RESONANT CURRENT-SOURCE CONVERTER

A. The Hard-Switched Current-Source Converter

The circuit operation of the Parallel-Resonant Current-Source Converter is based on the hard-switched Current-Source Converter (Fig. 15). Unlike voltage-source converters which inject pulsating current into the energy source or harmonics into the line, current-source converters draw a constant current from the supply.

A high input inductance transforms the voltage-source into a current-source. Current flowing through the input inductor changes at a slow rate and can be assumed constant for high frequency of operation. The current-source characteristics of the input provides a natural protection against short-circuits by averting sudden increase of current. The transformer provides electric isolation and voltage level shifting. Switches S_1 and S_2 are power semiconductor devices with reverse-blocking capability. MOSFETs or IGBTs devices are commonly used in the higher frequency range because of their fast switching speeds. In the Current-Source Converter however, MOSFETs or IGBTs must be connected in series with fast-recovery diodes that disable the internal body-drain diode of those devices [14] . The active switches S_1 and S_2 are connected to ground, thus making driver circuits for those devices fairly simple. Driver circuits can be designed without isolation transformer. The output stage of the hard-switched converter is a diode bridge rectifier with center-taps on the primary as well as on the secondary side. The minimum number of devices with this topology increases the reliability of the converter.
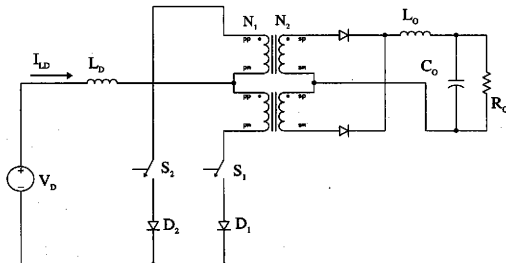
Fig. 15. The Current-Source Converter.

1. Operation of the Current-Source Converter

The operation of the circuit is described in this section. It is assumed that the converter is in steady-state.

<u>Mode I</u> : For $t_1 \le t \le t_2$, S_1 is on and S_2 off. The voltage across the primary side of the transformer is reflected on the secondary side (Fig. 16). Due to the negative and constant voltage across the inductor, its current decreases linearly.

<u>Mode II</u> : For $t_2 \le t \le t_3$, S_1 and S_2 are on. The transformer primary is shorted and across the inductor L_D lies a constant positive voltage of magnitude V_D. That voltage provokes a linear increase of the inductor current I_D which charges up the inductor with energy. Duty cycle D of switches S_1 and S_2 must be higher than 50% in order to
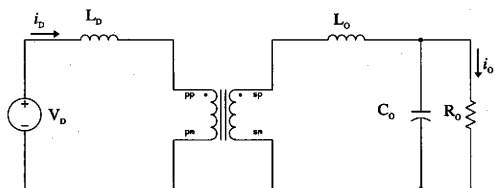
Fig. 16. Modes I and III of Current-Source Converter.
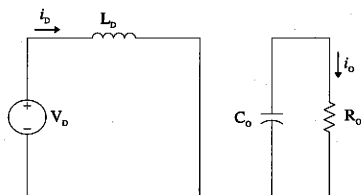
Fig. 17. Modes II and IV of Current-Source Converter.
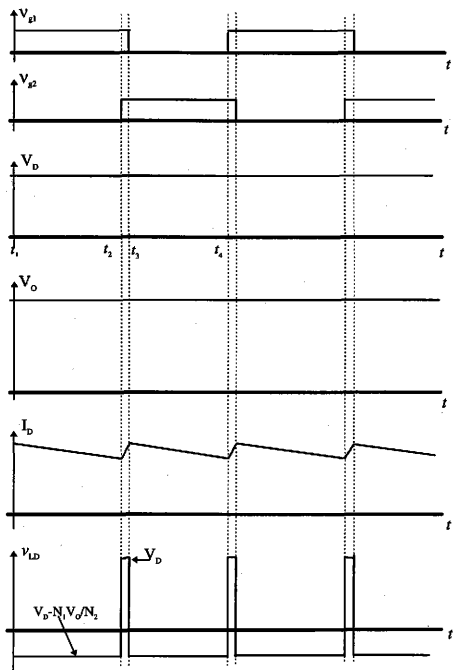
Fig. 18. Waveforms of Current-Source Converter.

maintain continuity of current in the inductor L_D (Fig. 17). Duty cycle less than 50% would cause an abrupt stop of current flow in the inductor and possibly lead to serious damages.

<u>Mode III</u> : For $t_3 \leq t \leq t_4$, S_1 is off while S_2 remains on. Apart from the change of voltage polarity across the transformer, this mode is similar to mode I.

<u>Mode IV</u> : For $t_4 \leq t \leq t_5$, S_1 and S_2 are on. This mode is similar to mode II .

Magnetic energy is stored in the inductor when both switches are on. Is a switch turned off, the magnetic energy stored in the inductor is added to the source energy and transferred to the load. The Current-Source Converter exhibits a characteristics typical of boost converters.

2. Analysis and Design

For analysis, it is assumed that the circuit elements are ideal and no power is dissipated in the transformer. Fig. 18 shows current and voltage waveforms of the Current-Source Converter in steady-state operation. In steady-state, the average voltage across the inductor L_D over a switching period must be zero:

$$\left[V_D - V_o \frac{N_1}{N_2} \right](1-D) = V_D \left(\frac{D-(1-D)}{2} \right) \qquad (4.1)$$

From (4.1), the output to input voltage ratio is:

$$\frac{V_o}{V_D} = \frac{N_2}{N_1} \frac{1}{2(1-D)} \qquad (4.2)$$

The Current-Source Converter uses PWM control and hard-switching. It has all the positive features of PWM converters including flexibility in control. It also experiences typical problems associated with PWM conversion such as limited frequency of operation, dangerous voltage spikes and high switching losses. In addition, it suffers from the high weight to voltage ratio due to the added choke inductor at the input [2]. Resonant power conversion offers a way to reduce the size and the losses of the converter without dramatic changes to the circuit. It also eliminates the dangerous voltage spikes caused by leakage inductances.

B. The Parallel-Resonant Current-Source Converter

The addition of a capacitor transforms the hard-switched Current-Source Converter into a resonant converter. The capacitor C_R is connected across the transformer on the primary side. Capacitor C_R forms a resonant tank with the transformer primary. The magnetizing inductance of the transformer is used as the resonant inductance of the LC tank. Leakage inductances of the transformer can be constructively included in the design of the converter.

The output stage of the converter consists of a diode bridge rectifier with LC filter. The filter reduces the ripple in the output voltage and maintains continuous mode of conduction in the rectifier. Electric isolation is achieved with a transformer. For balanced operation, the transformer must be symmetrical with respect to the center-tap. In the Current-Source Converter, the transformer has center-taps on the primary and secondary sides which divide them into 2 similar halves. At any given time, current flows in only one half on either side. The Parallel-Resonant Current-Source Converter has a center tap only on the primary side. At any given time, the resonant current flows in both halves of the transformer primary while the input current flows alternatively in one of both halves for a half-cycle.

1. Circuit Operation of the Resonant Converter

The switching sequence is similar to that of the hard-switched Current-Source Converter.

<u>Mode I</u> : for $t_1 \leq t \leq t_2$, S_1 is on and S_2 off. Current flows in switch S_1 and in the resonant tank (Fig. 19). In steady-state, the voltage across the capacitor is a sinewave. The duration of this mode is half of the resonant period. The capacitor voltage at the beginning and end of the mode is zero.

<u>Mode II</u> : for $t_2 \leq t \leq t_3$, S_1 and S_2 are on. The capacitor is short-circuited. The voltage across the capacitor is zero at the start of this mode and remains zero until end of the mode. S_2 is turned on at zero-voltage. Current increases in the inductor L_p and magnetic energy is stored in it. This mode is very short and lasts about 1% of the switching period. At the end of this mode, S_1 is turned off at zero voltage.

<u>Mode III</u> : for $t_3 \leq t \leq t_4$, S_1 is off and S_2 on. This mode is similar to mode I.

<u>Mode IV</u> : for $t_4 \leq t \leq t_5$, S_1 and S_2 are on. This mode is similar to mode II.

2. Time Domain Analysis of the Resonant Converter

2.1. Voltage Polarity across the Transformer

The resonant capacitor is connected across the transformer primary and sets the voltage on that side. In Fig. 20, a current flow into dot a means discharge of the capacitor and negative voltage across the transformer primary. The current on the
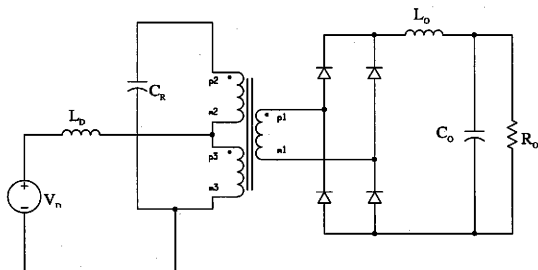
Fig. 19. Modes I and III of Parallel-Resonant Current-Source Converter.
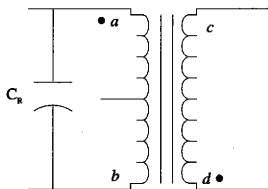
Fig. 20. Voltage Polarities across the Transformer.

secondary will therefore flow out of dot *d*. This establishes the dot rules for the transformer. The transformer reverses the polarity of the voltage.

2.2. AC Equivalent Circuit of the Diode Bridge Rectifier

The Parallel-Resonant Current-Source Converter consists of several stages. The first stage is an inverter that converts the DC input voltage into a sinewave across the transformer. The second stage is the transformer , the third stage a single phase diode bridge rectifier with output filter. The center-tap transformer is also part of the first stage. Operation of a single phase diode bridge rectifier is well known and covered in numerous literature [2,15] . The analysis of the circuit is considerably simplified if the rectifier-filter-load block is replaced by its equivalent AC resistance, assuming however that the voltage on the transformer secondary is an ideal sinewave [16,17]. Also harmonics content in the transformer secondary current is neglected. The model with the AC equivalent resistance does not include the effect of the output filter that can cause additional phase shift of the resonant voltage with respect to the resonant current.

2.3. AC Equivalent Resistance

The average output voltage of a single phase diode bridge rectifier in continuous conduction mode is:

$$V_{DC} = \frac{2\sqrt{2}}{\pi} V_{rms} \qquad (4.3)$$

Assuming that the power P_L is dissipated in the resistive load R_L connected on the output of the rectifier,

$$P_L = \frac{V_{dc}^2}{R_L} = \frac{8}{\pi^2} \frac{1}{R_L} V_{RMS}^2 \qquad (4.4)$$

An equivalent AC resistance R_{ac} directly connected across the sinusoidal voltage source dissipates the same amount of energy as the resistance R_L connected to the same source via the diode bridge rectifier.

$$P_L = \frac{V_{RMS}^2}{R_{ac}} \qquad (4.5)$$

From equations (4.4) and (4.5)

$$R_{ac} = \frac{\pi^2}{8} R_L \qquad (4.6)$$
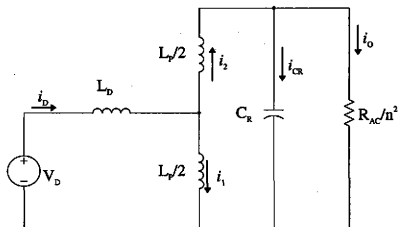
Fig. 21. Equivalent Circuit of Modes I and III (seen from Primary).

2.4. Analysis of Modes I and III

The transformer is replaced by its T-equivalent circuit. Leakage inductances and parasitic resistances are neglected. Because of the center-tap connection, the magnetizing inductance L_p is divided in 2 equal halves if the circuit is viewed from the primary side. The lower case letter n indicates the secondary to primary turns ratio. Analysis of mode I is sufficient since mode III is dual to mode I. Modes II and IV are too short and serve only as commutation intervals. The equivalent AC resistance of the output block is reflected on the primary side.

For mode I, a parallel resonant RLC structure is easily recognizable on Fig. 21. Loop and node equations yield:

$$V_d - \frac{L_p}{2}\frac{di}{dt} - L_d \frac{di_d}{dt} = 0 \qquad (4.7)$$

$$\frac{L_p}{2}\frac{di_1}{dt} - u_{CR} - L_p \frac{di_2}{dt} = 0 \qquad (4.8)$$

$$i_2 = i_o + i_{CR} \qquad (4.9)$$

$$u_{CR} = u_o = R_{ac} i_o \qquad (4.10)$$

$$i_{CR} = C_R \frac{du_{CR}}{dt} \qquad (4.11)$$

$$i_1 + i_2 = i_d \qquad (4.12)$$

After rearranging the terms, the following differential equation is obtained for the resonant capacitor voltage u_{CR}.

$$\frac{d^2 u_{CR}}{dt^2} + \frac{8n^2}{\pi^2} \frac{1}{R_L C_R} \frac{du_{CR}}{dt} + \frac{2L_D + L_p}{L_p + 4L_D} \frac{2}{L_p C_R} u_{CR} = \frac{2}{(L_p + 4L_D)C_R} V_D \quad (4.13)$$

In general $L_p \ll L_d$ and the equation becomes

$$\frac{d^2 u_{CR}}{dt^2} + \frac{8n^2}{\pi^2} \frac{1}{R_L C_R} \frac{du_{CR}}{dt} + \frac{1}{L_p C_R} u_{CR} = \frac{1}{2L_D C_R} V_D \quad (4.14)$$

(4.14) is a 2nd order differential equation with constant coefficients. The form of the solution is heavily influenced by the parameters R_L, C_R, L_p and n. The capacitor voltage can be either overdamped, critically damped or underdamped. 2 real and distinct roots of the characteristic equation of (4.14) yield an overdamped solution for the capacitor voltage, which is not desired. The parameter R_L, C_R, L_p and n must be chosen such that the solution of the differential equation (4.14) is an underdamped sinewave. The roots of the characteristic equation of (4.14) must be a complex conjugate pair. Those conditions are satisfied for $\omega_o > \alpha^2$ where ω_o and α are respectively the angular natural frequency and the damping factor of the parallel RLC circuit.

$$\omega_o = \frac{1}{\sqrt{L_p C_R}} = 2\pi f_o \quad (4.15)$$

$$\alpha = \frac{4n^2}{\pi^2} \frac{1}{R_L C_R} \quad (4.16)$$

In resonant circuits, the quality factor Q indicates the degree of purity of the sinusoidal form of resonant voltage and current. The quality factor is the ratio of the maximum energy stored in the resonant tank to the energy dissipated per resonant cycle.

$$Q = 2\pi \ \frac{\text{maximum energy stored}}{\text{energy dissipated per cycle}}$$

For the parallel resonant circuit of Fig. 21 , the quality factor is

$$Q_p = R\sqrt{\frac{C}{L}} = \frac{\pi^2}{8n^2}R_L\sqrt{\frac{C_R}{L_p}} \tag{4.17}$$

The value of the quality factor Q is critical to the design of resonant converters and must be high enough to produce acceptable sinusoidal waveforms, but not too high to produce high peak values in the resonant tank. The quality factor is chosen primarily as to improve the switching trajectory [18].

The switches S_1 and S_2 are operated at the natural frequency f_o of the parallel RLC circuit. For operation below resonance ($f_s < f_o$) , the parallel-resonant circuit represents an inductive load. Voltage across the switch is still positive after turn-off and negative before turn-on [14]. The switch begins the off-state with a positive voltage and ends with a negative voltage, producing high switching losses. For operation above resonance ($f_s > f_o$) , the parallel-resonant circuit represents a capacitive load. The switch begins the off-state with a negative voltage and ends with a positive voltage, also dissipating high switching losses. Basically, soft-switched operation occurs at the resonant frequency only. The voltage across the transformer and the resonant current are sinewaves of frequency f_o . At any time, the resonant current flows in the 2 halves of the transformer primary since they are integral part of the LC tank. In addition to

the resonant current, the DC input current flows through the lower half of the transformer primary in mode I or through the upper half in mode III.

At resonant frequency f_o , the maximun energy stored per cycle by the capacitive and inductive elements of the resonant tank are equal. L and C charge and discharge alternatively the same amount of energy . No reactive power is transferred between the resonant tank and either voltage source or load. The power delivered by the DC source is entirely consumed by the load (assuming ideal components).

3. Design of the Converter

The resonant capacitor sets the voltage on the primary side of the transformer. For continuous mode of conduction, the DC output voltage is tied to the peak of the voltage across the transformer secondary, which in turn depends on the peak voltage of the resonant capacitor and the turn ratio of the transformer. The peak voltage across the capacitor can be found by solving the differential equation (4.14). But this method involves complex analytical manipulations since the boundary conditions for voltage and current are not known a priori and have to be determined. Instead state-space averaging is very helpful for derivation of the converter voltage ratio. The use of state-space averaging is unusual in the design and the analysis of resonant converters. The presence of the choke inductor at the input of the converter makes it possible in this case. Fig. 22 shows waveforms of current and voltage of L_D and C_R.

In steady-state the average voltage across inductor L_D over a switching cycle must be zero. The center-tap divides the transformer primary in 2 parts of equal impedance. The voltage across a half of the transformer primary is always half the voltage across the resonant capacitor, whose peak value is V_{CRP}.
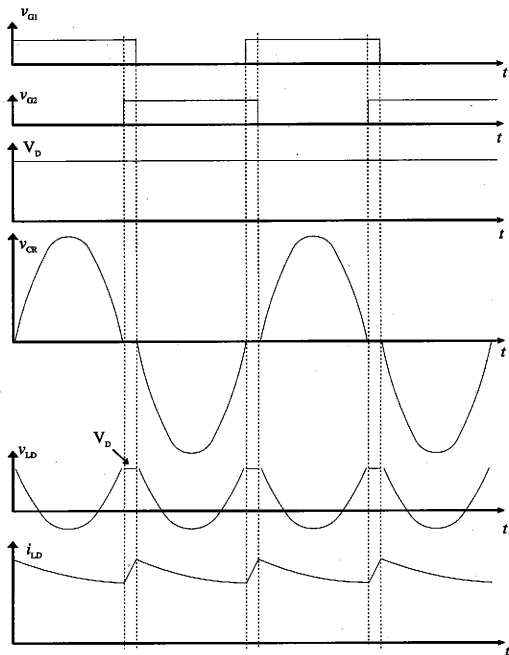
Fig. 22. Waveforms of the Parallel-Resonant Current-Source Converter.

$$\int_0^{(2D-1)T} V_D \, dt + \int_0^{(1-D)T} \left(V_D - \frac{V_{CRP}}{2} \sin \omega_o t \right) dt = 0 \qquad (4.18)$$

Solving the integrals yields:

$$V_D \left(D - \frac{1}{2} \right) + V_D (1-D) - \frac{V_{CRP}}{2} \frac{2}{\pi} (1-D) = 0 \qquad (4.19)$$

The peak resonant capacitor voltage is:

$$V_{CRP} = \frac{\pi}{2} \frac{1}{1-D} V_D \qquad (4.20)$$

The overlap time of the switches is very short and duty cycle D is approximately 50%. The peak voltage across the transformer primary is therefore:

$$V_{CRP} = \pi V_D \qquad (4.21)$$

The voltage on the secondary side of the center-tap transformer with turn ratio n is magnified by the factor n/2 The secondary side voltage is then approximated with the sinewave :

$$v_s = \frac{n}{2} \pi V_D \sin (2\pi f_o t) \qquad (4.22)$$

The voltage across the transformer secondary is rectified by a single phase diode bridge rectifier. Combining (4.3) and (4.22), the voltage ratio of the converter is :

$$\frac{V_o}{V_D} = n \qquad (4.23)$$

C. Frequency Domain Analysis

Analysis of the resonant converter in time domain deals only with operation at the resonant frequency. Switching frequency or duty cycle may change following disturbances such as variation of input voltage or circuit parameters. Frequency domain analysis covers a wider range of frequencies. Parasitic resistance of transformer and capacitors, which are important for efficiency estimation, can be included in this analysis.

In the basic circuit of the Parallel-Resonant Current-Source Converter, the resonant capacitor is on the primary side. The effect is unchanged if instead it is placed on the secondary side, or distributed on both sides of the transformer, as long as the equivalent capacitance is equal to C_R. Seen from the secondary side of the transformer, the input side of the circuit consisting of the source voltage V_D, the choke inductor L_D and the switches S_1 and S_2 can be modeled as a square-wave current-source of magnitude $\pm I_D/n$ (Fig. 23), where I_D is the constant input current and n the secondary to primary turn ratio of the transformer [14]. The output stage (rectifier, filter, load) is replaced by the equivalent AC resistance R_{ac}. The output voltage is determined by the peak voltage of the resonant circuit since continuous conduction of the bridge rectifier and sinusoidal waveform of the voltage across C_R are assumed. The input current for this model is described by:

$$i_i = \begin{cases} -\dfrac{I_D}{n} \text{ , for } 0 < \omega t \leq \pi \\[3mm] +\dfrac{I_D}{n} \text{ , for } \pi < \omega t \leq 2\pi \end{cases} \tag{4.24}$$

The Fourier analysis of the input current yields the fundamental rms value:

$$I_{i[RMS]} = \frac{2\sqrt{2}}{\pi\, n} I_D \tag{4.25}$$
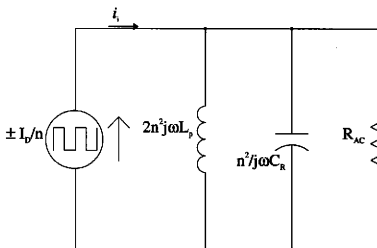
Fig. 23. Equivalent Circuit of Parallel-Resonant Current-Source Converter (seen from Secondary).

The admittance of the parallel-resonant circuit is expressed as

$$Y = \frac{1}{R_{ac}} + \frac{j\omega C_R}{n^2} + \frac{1}{n^2 j\omega L_P} = \frac{1}{R_{ac}} + \frac{j}{n^2}\left(\omega C_R - \frac{1}{\omega L_P}\right) \qquad (4.26)$$

The admittance is complex and has the magnitude:

$$|Y| = \sqrt{\frac{1}{R_{ac}} + \frac{1}{n^4}\left(\frac{\omega}{L_P\omega_o^2} - \frac{\omega_o^2 C_R}{\omega}\right)^2} \qquad (4.27)$$

The transfer function of the input current I_p to the rms voltage V_s of the parallel RLC resonant circuit is:

In ideal case, the converter has an efficiency of 100%. The power delivered by the source is totally dissipated in the resistance R_{ac} .

$$P_i = P_o \qquad (4.29)$$

Equation (4.29) expressed in terms of current and voltages yields:

$$V_D I_D = \frac{V_{s[RMS]}^2}{R_{ac}} \qquad (4.30)$$

Combining equations (4.28) and (4.30):

$$\frac{V_{s[RMS]}}{V_D} = \frac{n\pi}{2\sqrt{2}} R_{ac} |Y| \qquad (4.31)$$

From (4.3) and (4.31), the DC input to DC output voltage ratio is

$$\frac{V_o}{V_D} = nR_{ac} \sqrt{\frac{1}{R_{ac}^2} + \frac{1}{n^4}\left(\frac{\omega}{L_p \omega_o^2} - \frac{\omega_o^2}{\omega}C_R\right)^2} \qquad (4.32)$$

For operation at resonant frequency, $\omega = \omega_o$ and expression (4.32) becomes :

$$\frac{V_o}{V_D} = n \qquad (4.33)$$

Equations (4.33) and (4.23) have the same expression for the voltage ratio of the converter for operation at resonant frequency.

D. Devices Stresses

Semiconductor devices are subject to electrical and thermal limitations. A good estimate of semiconductor devices ratings is essential for any proper converter design.

1. Current Stresses

Due to the large choke inductor at the input and the high frequency of operation, the input current is nearly constant. Duty cycle of each switch is essentially 50% . For the ideal case of 100% efficiency, the input current is

$$I_D = \frac{P_o}{V_D} \qquad (4.34)$$

where P_o is the power delivered to the load and V_D the DC supply voltage. The current in switches S_1 and S_2 is a square-wave of magnitude I_D and duty cycle 50%. The rms current in switches S_1 and S_2 is therefore

$$I_{T(rms)} = \frac{1}{\sqrt{2}} \frac{P_o}{V_D} \qquad (4.35)$$

and the average current

$$I_{T(avg)} = \frac{1}{2} \frac{P_o}{V_D} \qquad (4.36)$$

In semiconductor devices, conduction losses are determined by both the magnitude and the shape of the current flowing through those devices.

Conduction losses in a semiconductor are estimated with the equation [10]:

$$P_{CON} = V_{TO}I_{T(avg)} + r_{T}I_{T(rms)}^{2} \qquad (4.37)$$

In the Parallel-Resonant Current-Source Converter, conduction losses in S_1 or S_2 are:

$$P_{CON} = \frac{1}{2} \frac{P_O}{V_D} \left(V_{TO} + r_T \frac{P_O}{V_D} \right) \qquad (4.38)$$

Equation (4.38) is also valid for the diodes D_1 and D_2 in series with the switches S_1 an S_2, if r_D and V_{TO} stand for on-state slope resistance and threshold voltage respectively.

2. Voltage Stresses

The switches S_1 and S_2 are rated at the peak voltage of the resonant capacitor, which is πV_D (2.41). The resonant nature of the waveforms naturally protects the circuit against overvoltages caused by leakage inductances in PWM converters.

3. Transformer Ratings

The design of a transformer is always a trade-off between size and efficiency [9]. Design of the transformer itself and choice of core material are beyond the scope of this thesis. Peak and rms values of the current flowing in the transformer are important design criteria and will be derived here. At resonant frequency, maximum resonant current in the transformer primary indicates zero capacitor voltage. Similarly when voltage across the capacitor is maximum, the resonant current is zero. The voltage

across the transformer primary is set by the resonant capacitor C_R. The peak and rms values of the resonant current are easily calculated if the characteristic impedance Z_R of the LC tank is known.

$$Z_R = \sqrt{\frac{L_P}{C_R}} \tag{4.39}$$

The peak and rms resonant current are:

$$I_{R[Peak]} = \frac{\pi V_D}{Z_R} \tag{4.40}$$

$$I_{R[RMS]} = \frac{1}{\sqrt{2}} \frac{\pi V_D}{Z_R} \tag{4.41}$$

In a switching cycle, the current in each half of the transformer primary consists of 2 segments, each lasting a half of a resonant period. One segment is shaped by the resonant current only while the other segment is formed by the resonant current with a DC offset, the input current. For operation at resonant frequency, the peak current in the transformer is equal to the peak resonant current.

$$I_{P(peak)} = I_D + I_{P[peak]} = \frac{P_O}{V_D} + \frac{\pi V_D}{Z_R} \tag{4.42}$$

The rms current flowing in the transformer primary:

$$I_{P[rms]} = \sqrt{\frac{1}{T} \left[\int_0^{\frac{T}{2}} \left(I_D - \sqrt{2} I_R \cos \omega_t t \right)^2 dt + \int_{\frac{T}{2}}^{T} \left(\sqrt{2} I_R \cos \omega_t t \right)^2 dt \right]} \tag{4.43}$$

where

$$T = \frac{2\pi}{\omega_0} \qquad (4.44)$$

Solving the integral in (4.43):

$$I_{P[RMS]} = \sqrt{\frac{1}{2}\left(2I_R^2 + I_D^2\right)} \qquad (4.45)$$

Expressed in terms of input voltage and output power, the current rms in the transformer primary is:

$$I_{P[RMS]} = \sqrt{\frac{1}{2}\left[\left(\frac{\pi V_D}{Z_R}\right)^2 + \left(\frac{P_O}{V_D}\right)^2\right]} \qquad (4.46)$$

The current rms through the transformer secondary is determined and easily calculated for a resistive load.

$$I_{S[RMS]} = \frac{2\sqrt{2}}{\pi}n\frac{V_D}{R_L} \qquad (4.47)$$

E. Control

The switching frequency of the Parallel-Resonant Current-Source Converter is the same as the resonant frequency of the tank. Zero-voltage switching is achieved by activating the switches at the zero-crossing of the resonant capacitor voltage, which occurs twice in a switching cycle. Turn-on and turn-off of the switches are both determined by the converter waveforms and not independently by the control circuit if

zero-voltage switching is desired. The converter loses 2 degrees of freedom with respect to conventional PWM converters. Operation off-resonance or change of duty cycle transfers the converter into hard-switching. The lack of flexibility in the control of the Parallel-Resonant Current-Source Converter results in poor output voltage regulation. The converter is not suitable for applications with frequent variations of input voltage.

The Parallel-Resonant Current-Source Converter in soft-switched operation is therefore a fixed frequency converter. The current-source characteristics of the converter does not allow duty cycle less than 50%. Since the converter operates at a duty cycle margin of 50%, a further reduction of duty cycle following an increase of input voltage is not recommended and may lead to operation failure of the converter. Output voltage regulation following a decrease of the input voltage can be achieved by increase of duty cycle, but with the penalty of higher switching losses since soft-switched operation is lost.

Although the Parallel-Resonant Current-Source Converter is basically a fixed frequency converter, a robust soft-switched control can be implemented such as to maintain lossless operation despite the variations of circuit parameters due to temperature for example. The control must include a zero-voltage detector for the resonant capacitor, that activates the turn-on of the non-conducting switch. The turn-off of the other switch occurs after a fixed delay, which represents the overlap time of the switches.

CHAPTER V

DESIGN EXAMPLE AND SIMULATION RESULTS

This Chapter presents a design example of a Parallel-Resonant Current-Source Converter. Leakage reactances are neglected. The specifications of the converter are as following:

> Input voltage V_D :   28 V
> Desired output voltage V_o: 4.5 kV
> Switching frequency f_s: 33 kHz
> Load resistance :   11250 Ω

From equation (4.21), the peak voltage across the resonant capacitor is

$$V_{CR[peak]} = \pi V_D = 3.14 * 28 = 87.96V \qquad (5.1)$$

Equation (4.25) gives the turn ratio of the transformer:

$$n = \frac{V_O}{V_D} = \frac{4500}{28} = 160.71 \qquad (5.2)$$

The resonant elements are derived from the switching frequency and the quality factor.

$$L_R C_R = \frac{1}{4\pi^2 f_S^2} = 2.326 * 10^{-11} \qquad (5.3)$$

Assuming a quality factor of .95 , the reactive elements are:

$$C_R = 8.68 \ \mu F \qquad L_R = 2.8 \ \mu H$$

A parasitic resistance of .44 Ω is assumed for the transformer primary.

Input inductance $L_D = 10$ mH

Output filter : $\qquad L_O = 10$ mH $\qquad C_O = 50 \ \mu H$

Characteristic impedance : $\quad Z_R \ = \ \sqrt{\dfrac{2.8}{8.68}} \ = \ 0.57 \ \Omega$ \qquad\qquad (5.4)

A digital computer simulation of this design example of a Parallel-Resonant Current-Source Converter is run on SunSPARC Station 20 using the simulation package Saber/PowerExpress from Analogy, Inc..

Input and output voltage are plotted on Fig. 24 and Fig. 25 . The output is a DC voltage with negligible ripple, just as the output current in Fig. 27. The low ripple in the output voltage and current is due to the high frequency of operation. The smooth input current is shown on Fig. 26.

Current in the switches S_1 and S_2 (Fig. 29) is a square-wave while the voltage across them is a half-sinewave (Fig. 28). Turn-on and turn-off of the switches are initiated at zero voltage, with no switching losses.

The voltage across the resonant capacitor has a sinusoidal form (Fig. 30) while the current consists of pieces of sinusoid (Fig. 31 and Fig. 32). The capacitor voltage is reflected on the secondary side with a reversal of polarity (Fig. 34). The current observed in the windings of the transformer secondary (Fig. 33) is typical of single phase diode rectifiers with LC output filter.
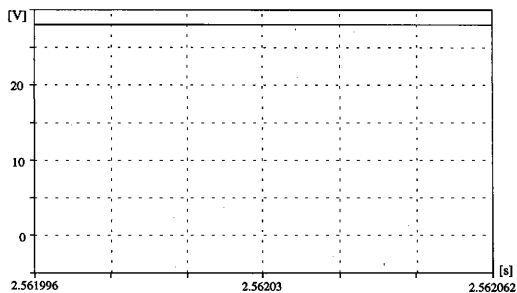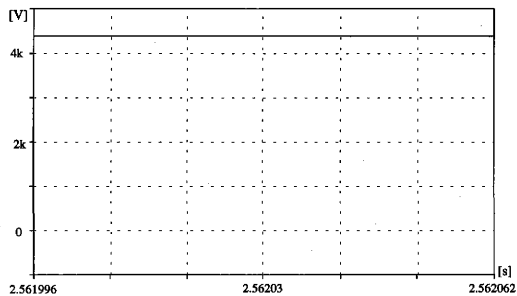
Fig. 24. Simulated Input Voltage.

Fig. 25. Simulated Output Voltage.
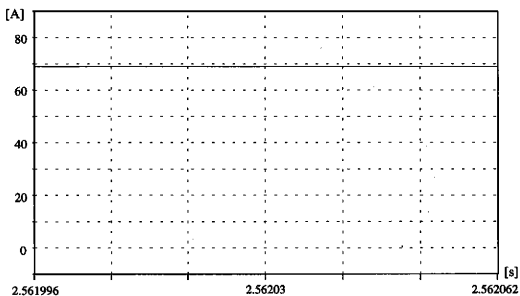
Fig. 26. Simulated Input Current.
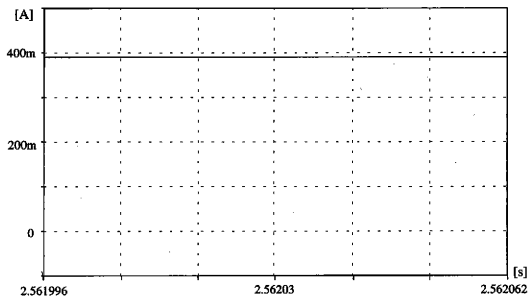
Fig. 27. Simulated Output Current.
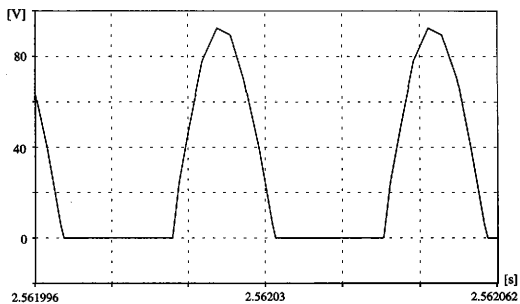
Fig. 28. Simulated Voltage across Switch S₁.
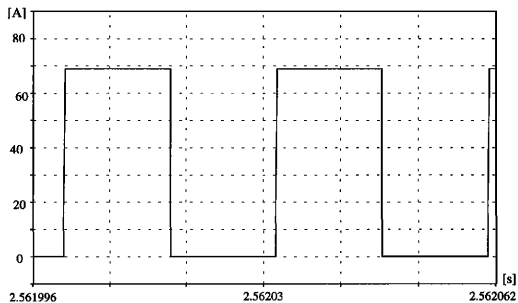
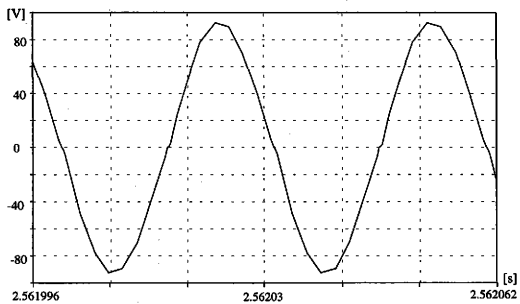Fig. 29. Simulated Current through Switch S₁.

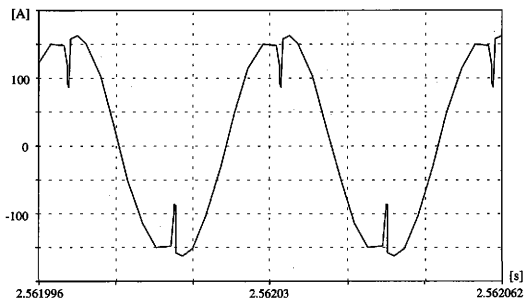Fig. 30. Simulated Voltage across Resonant Capacitor.

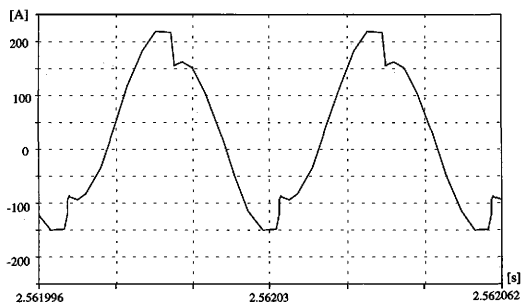Fig. 31. Simulated Current through Resonant Capacitor.

Fig. 32. Simulated Current through Transformer Primary.
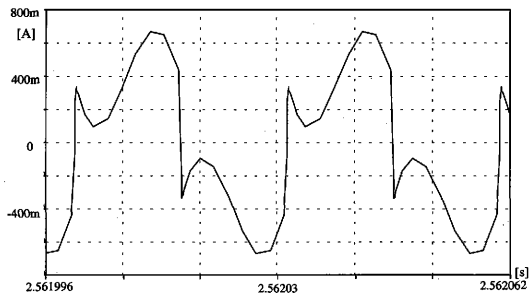
Fig. 33. Simulated Current through Transformer Secondary.
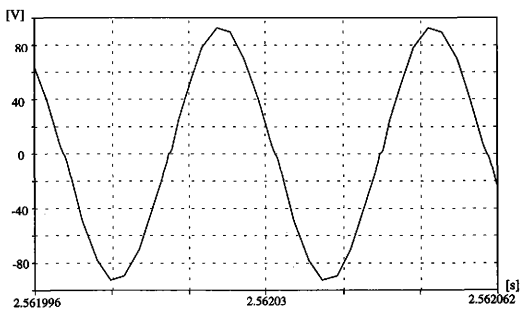
(a)
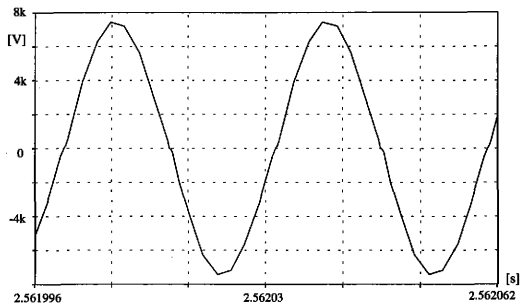
(b)

Fig. 34. Voltages across Transformer (a) Primary and (b) Secondary.

CHAPTER VI

EXPERIMENTAL RESULTS

A. Converter Specifications and Parameters

A prototype of the Parallel-Resonant Current-Source Converter was built and tested in the Power Electronics Laboratory at Texas A&M University. The converter is intended to supply a Microwave Electrothermal Thruster. The converter has to meet stringent requirements of space applications such as small weight, small volume and high efficiency. The specifications of the converter are:

Input voltage :	28 ±3 V
Output voltage :	4.5 kV
Output regulation :	less than 5%
Output power :	1.8 kW
Efficiency :	higher than 90 %
Peak output current :	1600 mA
Average output current :	400 mA
Packaging dimensions :	8.5" by 11"

The converter is designed following the same procedure as with the design example of Chapter V. However, due to practical considerations some changes are necessary. The transformer secondary consists of 6 isolated windings, which are each connected across a single phase diode bridge rectifier with output LC filter. Each transformer secondary has 27 times turns more than the transformer primary, giving a overall turn ratio of 162. The resonant capacitor is distributed on both sides of the transformer

because on the nonideality of the transformer and the need to eliminate overvoltage due to leakage inductances. The output of the 6 rectifiers are connected in series. The series connection is necessary since output voltage is higher than the rating of each bridge rectifier. Equal distribution of the output voltage across the rectifiers is achieved with a resistor bank. The transformer primary consists of circular copper bars of relative large area. The large area facilitates the flow of the high current on the primary side. The input inductance is higher than in the design example of Chapter V. In the design example of Chapter V, a smaller inductance value was chosen to allow a faster convergence of the simulation towards steady-state. The following components are used.

Resonant capacitance :	8.36 µF
Transformer primary inductance :	2.78 µH
Transformer turns ratio :	160.71
Nominal resonant frequency :	33 kHz
Nominal quality factor :	.75
Transformer primary resistance :	.44 Ω
Input inductance :	87.1 mH
Input filter inductance :	3.47 µH
Input filter capacitance :	3000 µF
Output filter inductance :	81.41 mH
Output filter capacitance :	.22 µF

Switches S_1 and S_2 are realized each with 3 IGBTs APT20M25JNR connected in parallel to increase the current capability of the switch. Power diodes MBR30060CT of Motorola are connected in series with each switch. Each output rectifier stage consists of 8 diodes MUR4100E-9324 of Motorola. 2 diodes are connected in series to match the voltage rating of the bridge rectifier.

B. Converter Waveforms

Fig. 35 shows unfiltered and filtered voltage across one rectifier of the output stage, which is 1/6 of the total output voltage. Gating signal and voltage across one of the active switches are plotted on Fig. 36. Turn-on occurs at zero-voltage while at turn-off, there is still some positive voltage across the switch, producing some turn-off losses. Voltage across and current through the transformer primary are plotted Fig. 37. The voltage across the transformer primary is near sinusoidal while the current clearly exhibits a 3rd harmonics component. This is due to the DC offset that is present for half of the cycle. The frequency of operation of the converter is 26.24 kHz instead of the nominal 33 kHz. During operation, circuit parameters such as resonant frequency change due to temperature. The switching frequency is adjusted accordingly since the control circuit senses the zero-voltage crossing of the resonant voltage.
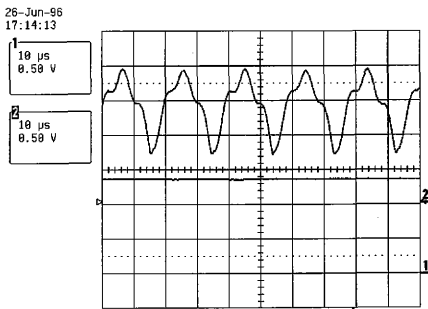

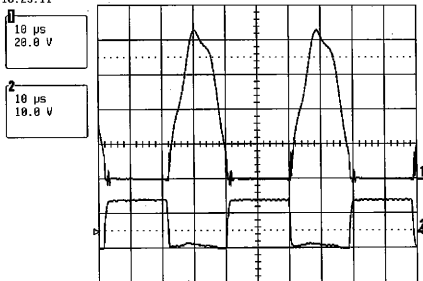Fig. 35. Unfiltered (2) and Filtered (1) Output Voltage.

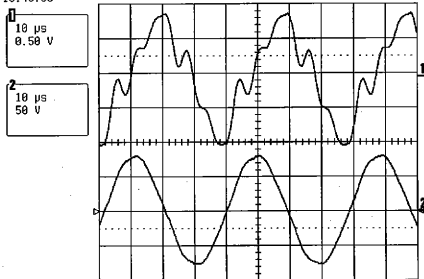Fig. 36. Voltage across Switch S_1 (1) and Gating Signal (2).

Fig. 37 . Transformer Primary Current (1) and Voltage (2).

C. Measurement Procedure

All measurements are approximations of true value. There are no perfect or absolutely accurate measurements [19]. The difference between the measured value and the true value is the error of the measurement. Generally measurement errors fall into 3 categories: random error, gross error and systematic error. Gross errors are people caused errors. They include false reading, wrong connection, wrong meter, wrong scale, wrong interpolation, wrong probes, etc....Systematic errors are equipment errors. They are related to terms such as accuracy, precision, calibration and tolerance. Random errors are nonpredictable and obey the laws of probability. Errors are minimized when instead of just one reading, a series of measurement is performed.

For the readings, digital multimeters FLUKE 87 and TEK DM254 are used. The accuracy of those instruments for measurements of DC and AC voltage, DC and AC current, resistance, frequency and duty cycle is less or equal to 1%. The output voltage is measured with the high voltage probe FLUKE 80K-6 which has an accuracy of ±1% for DC voltage. To check the accuracy of the readings, the output voltage is also obtained by measuring the voltage of each rectifier output without the probe, and then adding them. The input current is measured with the clamp-on AC/DC current probe FLUKE Y8100 with a DC current accuracy of ±2% of 200A, or 4A. The accuracy of the instruments indicates the number of significant digits of the multimeter display.

For each quantity, a series of 5 measurements is performed. The mean value of the readings is taken as the true value of the measurement while the standard deviation indicates the probable error. The standard deviation is given by the formula :

$$\sigma = \sqrt{\frac{\sum_{i=1}^{n} d_i^2}{n-1}} \qquad (6.1)$$

where d_i represents the deviation of the *ith* measurement from the mean value and n the number of readings in a measurement series. The standard deviation is widely used in error analysis [19]. The smaller the standard deviation is, the more precise is the measurement.

D. Propagation of Errors

Power and efficiency are not measured directly, but derived from the quantities current and voltage. Direct measurements are not perfect and contain errors that are propagated during calculations [20]. The numbers $A + a$ and $B + b$ are given, where the capital letter represents the true value and the lower case letter the error.

1. Multiplication of Numbers

The multiplication of the numbers defined above yields:

$$(A + a) \cdot (B + b) = AB + Ab + aB + ab \qquad (6.2)$$

Errors a and b are small. Thus the term ab becomes too small with respect to aB, bA, A or B and may be neglected. The absolute error is approximately

$$e \ = \ Ab + aB \qquad (6.3)$$

and the relative error

$$m \ = \ \frac{aB + bA}{AB} \ = \ \frac{a}{A} + \frac{b}{B} \qquad (6.4)$$

2. Division of Numbers

The division of the 2 numbers yields

$$\frac{A+a}{B+b} = \frac{A+a}{B\left(1+\dfrac{b}{B}\right)} = \frac{A+a}{B}\left[1-\frac{b}{B}+\left(\frac{b}{B}\right)^2 \cdots\right] \qquad (6.5)$$

Terms to the power of 2 or higher may be neglected. Equation 6.5 becomes

$$\frac{A+a}{B+b} \approx \frac{A+a}{B}\left(1-\frac{b}{B}\right) = \frac{A}{B}+\frac{a}{B}\left(1-\frac{b}{B}\right)-\frac{Ab}{B^2} \qquad (6.6)$$

The absolute error is calculated as

$$e = \frac{a}{B}\left(1-\frac{b}{B}\right)-\frac{Ab}{B^2} \approx \frac{a}{B}-\frac{Ab}{B^2} \qquad (6.7)$$

and the relative error

$$m = \frac{a}{A}-\frac{b}{B} \qquad (6.8)$$

Equations 6.3 and 6.7 are used to determine the absolute error of the measurement while equations 6.4 and 6.8 yield the relative error for power and efficiency. The lower letter cases a and b represents in this case the standard deviation of any measurement series.

E. Efficiency Results

The values of input current, output current and output voltage are reported in Table 1 for input voltages ranging from 22 V to 28 V. Relative errors of measurements are also reported. Relative errors are calculated as the ratio of absolute error or standard deviation to the mean value of each measurements series.

Table 1 . Voltages and Currents.

V_D	I_D	V_o	I_o
[V]	[A]	[V]	[mA]
22	51.92 ± 1.6%	3277 ± .1%	306 ± .1%
23	54.16 ± 1.5%	3428 ± .1%	320 ± .2%
24	56.46 ± 1.5%	3580 ± .4%	334 ± .1%
25	58.94 ± 1.3%	3735 ± .2%	348 ± .2%
26	61.12 ± 1.5%	3887 ± .2%	362 ± .2%
27	63.32 ± 1.6%	4041 ± .1%	377 ± .3%
28	65.9 ± 1.3%	4193 ± .1%	391 ± .2%

Input power P_{IN}, output power P_o and efficiency η of the converter are reported in Table 2. The efficiency of the converter is around 89% for input voltage ranging from 22 V to 28 V (Fig. 38) with errors of approximately 1% (Table 2). Conduction losses on the primary side account for most of the energy dissipated in the converter. For input voltages in that range, the input current is higher than 52 A while the current rms in the transformer primary is around 46 A. As matter of illustration, a transformer with

Table 2 . Power and Efficiency.

V_D	P_{IN}	P_O	η
[V]	[W]	[W]	[%]
22	$1142 \pm 1.6\%$	$1003 \pm .2\%$	$88 \pm 1.4\%$
23	$1246 \pm 1.5\%$	$1097 \pm .3\%$	$88 \pm 1.2\%$
24	$1355 \pm 1.5\%$	$1196 \pm .2\%$	$88 \pm 1.3\%$
25	$1474 \pm 1.3\%$	$1300 \pm .4\%$	$88 \pm .9\%$
26	$1589 \pm 1.5\%$	$1407 \pm .5\%$	$89 \pm 1\%$
27	$1710 \pm 1.6\%$	$1523 \pm .4\%$	$89 \pm 1.2\%$
28	$1845 \pm 1.3\%$	$1639 \pm .3\%$	$89 \pm 1\%$
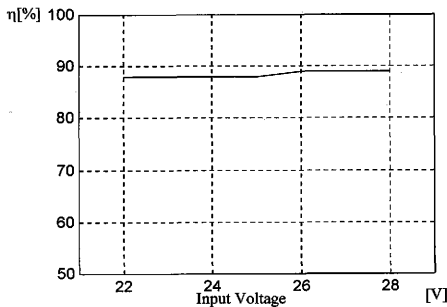
Fig. 38. Converter Efficiency.

a parasitic resistance of .05Ω would dissipate almost 106 W in ohmic losses, more than half of the total losses. Other sources of losses are the forward resistance of the IGBTs and the diodes. Diodes provide reverse-blocking capability for the switches, but they also increase the resistance of the current path and account for a few percents of power dissipated in the converter. Given the magnitude of the currents on the primary side, an efficiency of 89 % suggests that switching losses have been kept to a minimum.

The hall-sensor current probe has been a major source of concern by the evaluation of the converter. But the values of input current obtained with the probe FLUKE Y8100 have been confirmed by measurements with a analog DC current meter from Simpson Electric Corporation.

CHAPTER VII

SUMMARY AND CONCLUSIONS

A. Summary

A new DC-DC converter topology, the Parallel-Resonant Current-Source Converter, has been presented in this thesis. A large choke inductor at the input of the converter transforms the voltage-source into a current-source, which provides an inherent protection against short-circuits. The active switches are connected to ground, thus considerably simplifying their gate or base drive circuit. Instead of the leakage inductance, the magnetizing inductance is used as the resonant inductance of the LC tank. The center-tap transformer assumes the functions of resonant inductance, electric isolation and voltage level shifting. The parallel structure of the LC tank restricts the oscillating current within the resonant tank. The most important feature of this converter however is the soft-switched operation, which yields a high efficiency and allows a drastic reduction of the size of the converter. The voltage ratio of the converter is determined solely by the turns ratio of the transformer. Simulation and experimental results have confirmed the occurrence of zero-voltage switching while efficiency around 90% have been recorded for a 1.8 kW prototype.

Reduced electromagnetic interference (EMI) is another benefit of this converter topology. The current-source nature of the input prevents a pulsating current from flowing in the main DC bus and the resonant waveform of the voltage limits high dv/dt production, which are important source of noise. Shielding of small-signal circuits becomes obsolete. This results in further reduction of size, cost savings and less complexity for the setup.

The main drawback of this converter however is the lack of flexibility in the control. Soft-switched output voltage regulation is quasi impossible with this converter.

B. Critique of the Analysis

Ideal electrical components have been assumed throughout the analysis of the Parallel-Resonant Current-Source Converter. The addition of the parasitic resistances of transformer, semiconductor devices and capacitors can notably alter the peak values of resonant voltage and current and complicate the time domain analysis of the converter. However inclusion of these resistances is easy in the frequency domain analysis and would give better efficiency estimation. Also the single phase diode rectifier in the output stage of the converter has been replaced by an AC equivalent resistance. Analysis with the AC equivalent resistance is accurate as long as only real power transfer is of importance. The model with the AC equivalent resistance does not include the effect of the output LC filter which may provoke an additional phase shift of the resonant voltage and change the resonant frequency of the converter. The additional phase shift may transfer the converter into hard-switching.

C. Future of Resonant Power Conversion

Resonant power conversion solves many problems associated with linear or square-wave converters such as abundant switching losses, high peaks and electromagnetic interference (EMI) . However new problems are created as the old ones are solved. New problems include higher demands on magnetic design, cooling and control issues.

The smooth curves produced by resonant techniques neutralize the negative effect of leakage inductances. In fact, parasitic inductances are positively included in the design of the resonant elements. For the designer, it means that the core shape and the physical dimensions of the transformer are not geared towards low leakage inductance. Instead, the higher peak and rms currents emphasize other issues like capacitor, winding and core losses. Although resonant converters must still satisfy basic requirements common to all converters, the approach in the design is different.

Cooling is another challenge resulting from the emergence of resonant converters. Heat produced by the losses must be transferred out of the converter. Resonant power conversion is aimed at the reduction of the size of the converter. The smaller size of the converter further reduces the area available for heat transfer, which is facilitated by a large area. But thermal constraints dominate frequency constraints because device are easily damaged by overheating. A design alternative is to build converters with large surface-to-volume ratios [5]. A reasonable heat transfer can still be achieved while maintaining the small weight of the converter. This suggests a break away from the traditional cubic form of the magnetics.

But improvements in control strategies remain the greatest challenge of resonant power conversion. Conventional methods such as state-space averaging fail while analytical methods do not produce meaningful results. The gains achieved in terms of efficiency do not always offset the added control complexity, which considerably reduces the range of applicable loads. The constant decrease in the cost of silicon and the increased integration of functions on a single chip will certainly galvanize the development of unconventional control strategies optimized for resonant power conversion. Resonant power conversion is a practical and viable technology, not only for aerospace applications

REFERENCES

[1] K. Kit Sum, "The development of resonant power conversion," *Recent Developments in Resonant Power Conversion*, pp. 3-19, Intertec Communications, Inc., Ventura, California, 1988.

[2] N. Mohan, T. Undeland, W. Robbins , *Power Electronics: Converters, Applications and Design*, 2nd ed., John Wiley & Sons, Inc., New York, 1995.

[3] Odon Ferenczi, *Power Supplies : Part B*, Elevier, Amsterdam, Oxford, New York, 1987.

[4] Yim-Shu Lee, *Computer-Aided Analysis and Design of Switch-Mode Power Supplies*, Marcel Dekker, Inc., New York, 1993.

[5] Steve Freeland, "An introduction to the principles and the features of resonant power conversion," *Recent Developments in Resonant Power Conversion*, pp. 20-43, Intertec Communications, Inc., Ventura, California, 1988.

[6] F.C. Lee, K. Liu, "Zero-voltage switching technique in dc-dc converters," *IEEE Power Electronics Specialist Conference*, pp. 58-70, Vancouver, British Columbia, June 23-27, 1886.

[7] F. Tsai, J. Sabate, F.C. Lee, "Constant-frequency, zero-voltage switched, clamped-mode parallel-resonant converter," *11th Int. Telecommunications Energy Conference*, Firenze, Italy, 1989.

[8] M.J. Fisher, *Power Electronics*, PWS-Kent Publishing Company, Boston, 1991.

[9] T. McLyman, *Transformer and Inductor Design Handbook*, Marcel Dekker, Inc., New York, 1978.

[10] K. Heumann, *Grundlagen der Leistungselektronik*, Springer, Berlin, 1985.

[11] D.M. Divan, "The resonant dc link converter- A new concept in static power conversion," *IEEE Transactions on Industry Applications*, vol. 25, no. 2, pp. 317-325, March/April 1989.

[12] L. Laskai, T.S. Wu, M. Ehsani, "Inductor coupled converter (IC^2) for high power dc-dc applications," *IEEE Power Electronics Specialists Conference*, pp. 1085-92, Toledo, Spain, 1992.

[13] L. Laskai, M. Ehsani, "The zero-switching loss mechanism in the capacitor coupled converter (C^3) and its extensions," *IEEE Industry Applications Society Conference Records*, pp. 910-17, Houston, Texas, 1992.

[14] M.K. Kazimierczuk, R.C. Cravens II, "Current-source parallel-resonant dc/ac inverter with transformer," *IEEE Transactions on Power Electronics*, vol. 11, no. 2, pp. 275-84, March 1996.

[15] M. Rashid, *Power Electronics: Circuits, Devices and Applications*, 2nd edition, Prentice Hall, Englewood Cliffs, New Jersey, 1993.

[16] A. Bhat, "Fixed-frequency PWM series-parallel resonant converter," *IEEE Transactions on Industry Applications*, vol. 28, no. 5, pp. 1002-09, Sept/Oct 1992.

[17] A. Bhat, "Analysis and design of a fixed frequency LCL-type series resonant converter," *IEEE Applied Power Electronics Conference and Exposition*, pp. 253-60, Boston, Massachusetts, 1992.

[18] I. J. Pitel, "Phase-modulated resonant power conversion techniques for high-frequency link inverters," *IEEE Transactions on Industry Applications*, vol. 22, no. 6, pp. 1044-51, Nov/Dec 1986.

[19] L. M. Thompson, *Basic Electrical Measurements and Calibration*, Instrument Society of America, Pittsburgh, Pennsylvania, 1979.

[20] J.E. Gibson, *Introduction to Engineering Design*, Holt, Rinehart and Winston, Inc., New York, 1968.

VITA

Aristide-Marie Tchamdjou received his "Diplom" in Electrical Engineering from the "Technische Universitaet Berlin", Germany, in October 1992. After spending one semester as non-degree graduate student at Iowa State University during Fall 1993, he joined the graduate program in electrical engineering at Texas A&M University, College Station, June 1994. His research areas include power electronics, motor drives and their control. He can be reached at : International Rectifier, 233 Kansas Street, El Segundo, CA 90245-4382 .Tel : (310) 252-7031 , Fax : (310) 252-7171 .